Supplementary Information

Room-Temperature-Modulated Polymorphism of Nonfullerene Acceptors Enable Efficient Bilayer Organic Solar Cells

Zhenmin Zhao [1], Sein Chung [2], Young Yong Kim [3], Minyoung Jeong [2], Xin Li [1], Jingjing Zhao [1], Chaofeng Zhu [1], Safakath Karuthedath [4], Yufei Zhong [5], Kilwon Cho [2], Zhipeng Kan [1*]

[1] Center on Nanoenergy Research, Guangxi Colleges and Universities Key Laboratory of Blue Energy and Systems Integration, Institute of Science and Technology for Carbon Peak & Neutrality, School of Physical Science & Technology, Guangxi University, Nanning 530004, China

[2] Department of Chemical Engineering, Pohang University of Science and Technology, Pohang 37673, South Korea.

[3] Beamline Division, Pohang Accelerator Laboratory, Pohang University of Science and Technology, Pohang 37673, Republic of Korea.

[4] Institute of Materials Research, Tsinghua Shenzhen International Graduate School, Tsinghua University, Shenzhen, 518055 China.

5 Zhejiang engineering research center for fabrication and application of advanced photovoltaic materials, School of Materials Science and Engineering, NingboTech University, No.1 Qianhu South Road, Ningbo 315100, People's Republic of China.

* Corresponding author, E-mail: kanzhipeng@gxu.edu.cn

Content

1. Experimental Section/Methods

Materials. PM6, Y6, and BTP-eC9 were purchased from Solarmer Co., Ltd. (Beijing, China). PEDOT: PSS and PDIN were purchased from Energy Chemical., Ltd. These materials were used as received without further treatment.

Device Fabrication. Bilayer organic solar cells were prepared on glass substrates with tin-doped indium oxide (ITO, 15 Ω/sq) (device area: 0.04 cm^2). Substrates were prewashed with isopropanol to remove organic residues before immersing them in an ultrasonic bath of soap for 15 min. Samples were rinsed in flowing deionized water for 5 min before being sonicated for 15 min each in successive baths of deionized water, acetone, and isopropanol. Next, the samples were dried with pressurized nitrogen before being exposed to a UV-ozone plasma for 15 min. A thin layer of PEDOT:PSS (~20 nm) (Clevios AL4083) was spin-coated onto the UV-treated substrates, the PEDOT-coated substrates were subsequently annealed on a hot plate at 150 °C for 20 min, and the substrates were then transferred into the glovebox for active layer deposition.

All solutions were prepared in the glovebox using the PM6 and NFAs Y6 and BTP-eC9 donors. Optimized devices were obtained by dissolving PM6 in chloroform (CF) using a concentration of 8 mg/ml, and NFAs were dissolved in dichloromethane (DCM) with and w/o additives (The volume fraction of FN, CN, and BN are 0.9%, 0.5%, and 0.6%, respectively). Note: The NFA solutions were stirred for three hours at 50 °C before being cast. For the solar cells with a bilayer architecture, PM6 was bladed on the PEDOT: PSS layer to form a front layer, and then NFAs with and w/o additives were bladed onto the donor layer. Then, a methanol solution of PDIN at a concentration of 2.0 mg/ml with acetic acid (0.3 vol%) added as a processing additive was spin-coated onto the active layer at 5000 rpm.

Next, the substrates were pumped down in a high vacuum at a pressure of 3×10^{-4} Pa, and the Ag layer (100 nm) was thermally evaporated onto the active layer.

Photocurrent measurements. The J−V measurement was performed via a XES-50S1 (SAN-EI Electric Co., Ltd.) solar simulator (AAA grade) whose intensity was calibrated by a certified standard silicon solar cell (SRC-2020, Enlitech) under the illumination of AM 1.5G 100 mW cm^{-2}. The AM 1.5G light source with a spectral mismatch factor of 1.01 was calibrated by the National Institute of Metrology. The intensity of the AM 1.5G spectra was calibrated by a certified standard silicon solar cell (SRC-2020, Enlitech) calibrated by the National Institute of Metrology. The J-V curves of small-area devices were measured in forwarding scan mode (from -0.2 V to 1.2 V) with a scan step length of 0.02 V. The external quantum efficiency (EQE) was measured by a certified incident photon to electron conversion (IPCE) equipment (QE-R) from Enli Technology Co., Lt. The light intensity at each wavelength was calibrated using a standard monocrystalline Si photovoltaic cell. Optoelectronic characterizations were performed with PAIOS (Fluxim, Switzerland).

2. PL spectra of Y6 films

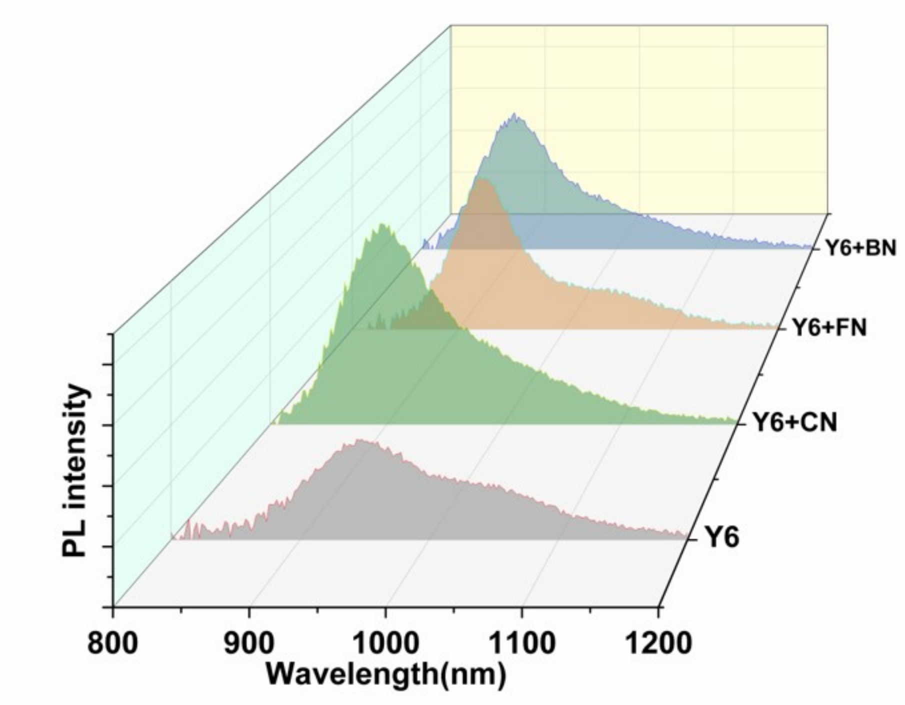

Figure S1. PL spectra of Y6, Y6(CN), Y6(FN) and Y6(BN).

3. In-situ absorption

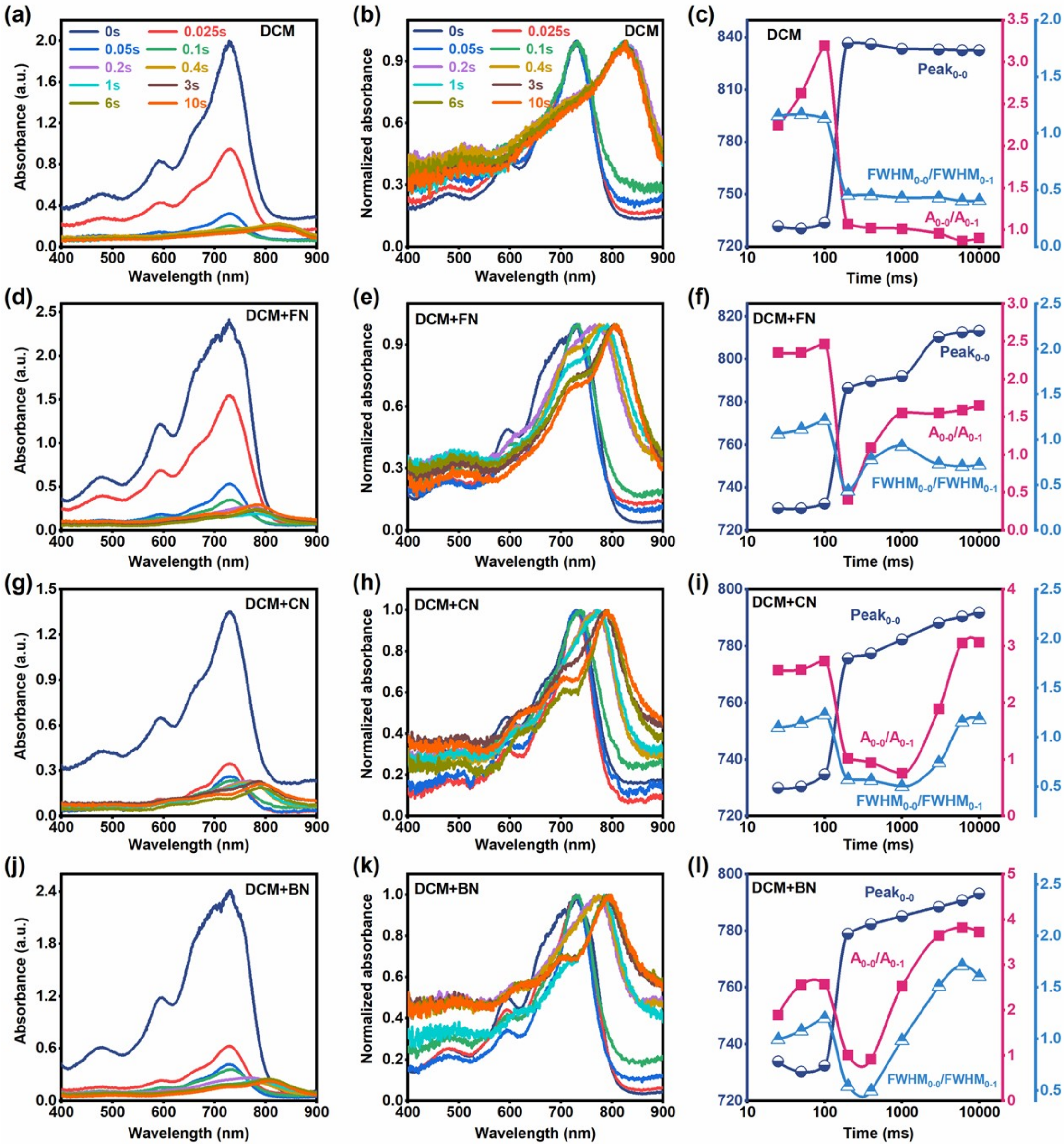

Figue S2. In-situ absorption spectra of **a)** Y6, **d)** Y6+FN, **g)** Y6+CN, **j)** Y6+BN films. Normalized transient absorption spectra of **b)** Y6, **e)** Y6+FN, **h)** Y6+CN, **k)** Y6+BN films. Values of $FWHM_{0\text{-}0}/FWHM_{0\text{-}1}$, $A_{0\text{-}0}/A_{0\text{-}1}$, and $Peak_{0\text{-}0}$ of **c)** Y6, **f)** Y6+FN, **i)** Y6+CN, **l)** Y6+BN films change with drying time.

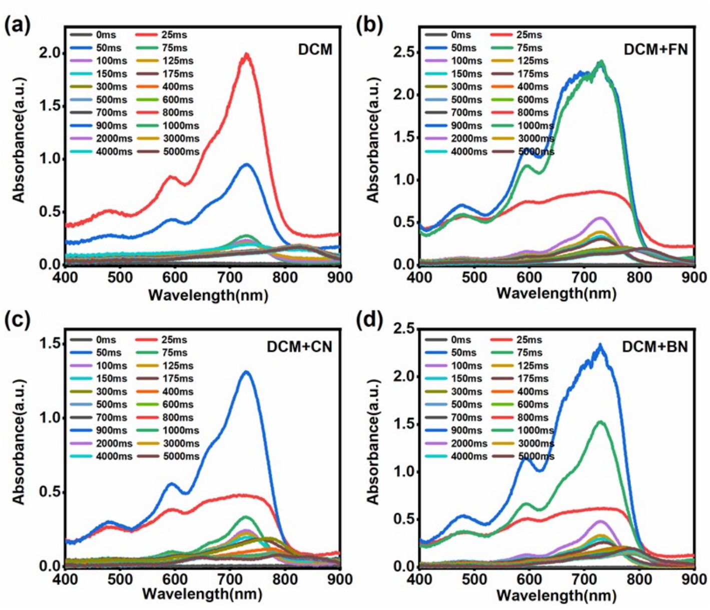

Figure S3. In-situ absorption spectra (0-5s) of **a)** Y6, **b)** Y6+FN, **c)** Y6+CN, **d)** Y6+BN films.

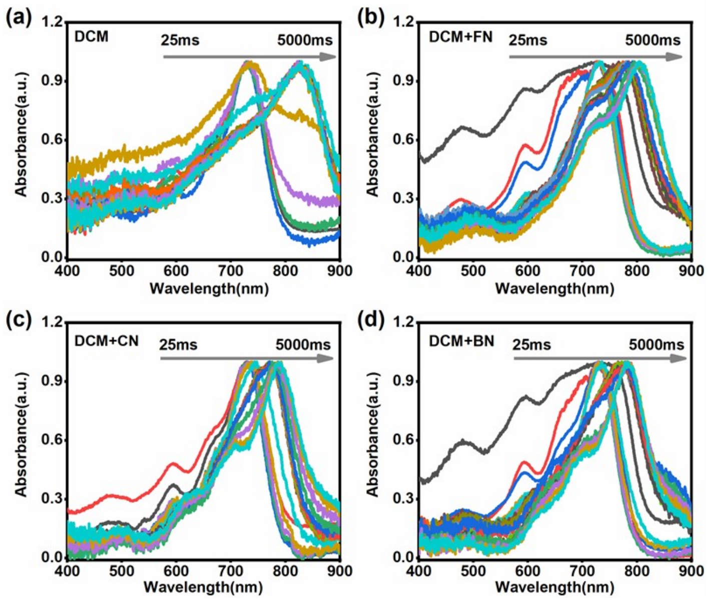

Figure S4. Normalized in-situ absorption spectra (0-5s) of **a)** Y6, **b)** Y6+FN, **c)** Y6+CN, **d)** Y6+BN films.

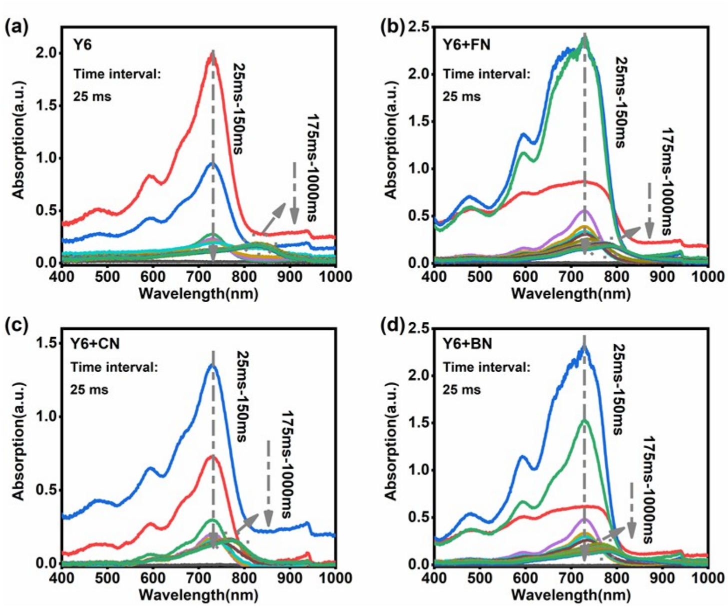

Figure S5. In-situ absorption spectra (0-1s, 40 points) of **a)** Y6, **b)** Y6+FN, **c)** Y6+CN, **d)** Y6+BN films.

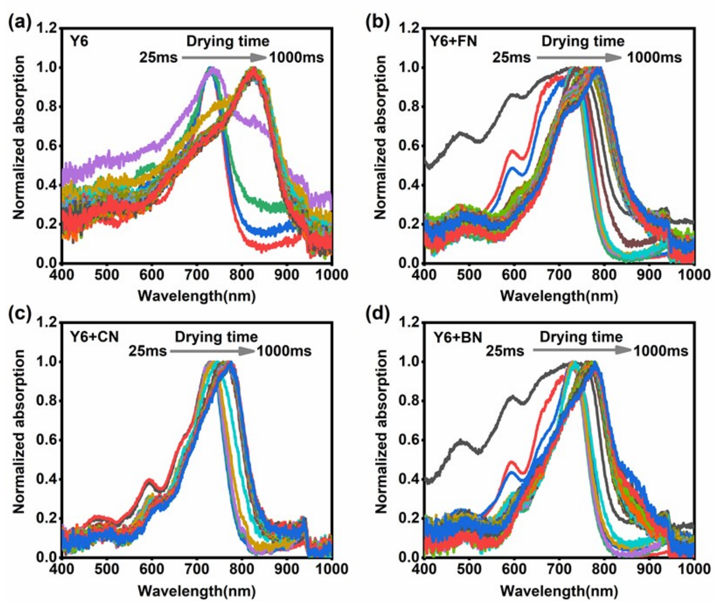

Figure S6. Normalized in-situ absorption spectra of **a)** Y6, **b)** Y6+FN, **c)** Y6+CN, **d)** Y6+BN films.

4. Film thickness of PM6/Y6 films

Table S1 │ Film thickness of PM6/N3. The sum of the thickness of single donor and acceptor films is consistent with that of the bilayer device.

Materials	Solvent	Concentration (mg/ml)	Thickness[a] (nm)
PM6	CF	8	57±2
Y6	DCM	10	40±4
	DCM+CN	10	51±5
	DCM+FN	10	50±3
	DCM+BN	10	43±2
PM6/Y6	CF/DCM	8/10	98±1
	CF/DCM(CN)	8/10	107±3
	CF/DCM(FN)	8/10	110±4
	CF/DCM(BN)	8/10	98±2

[a] The average values obtained from 5 films for each condition.

5. AFM measurements of Y6 in DCM

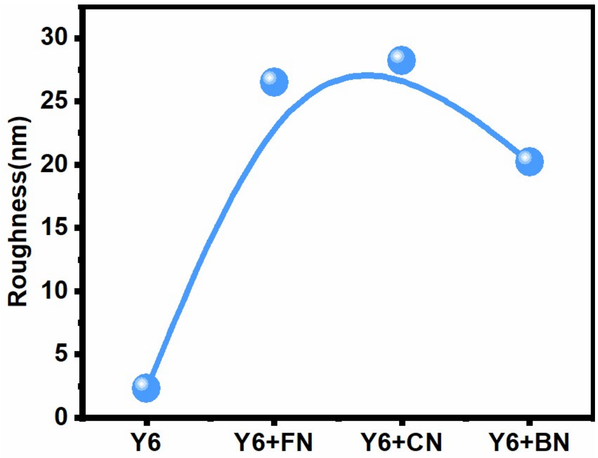

Figure S7. Roughness of Y6 films changed with additives.

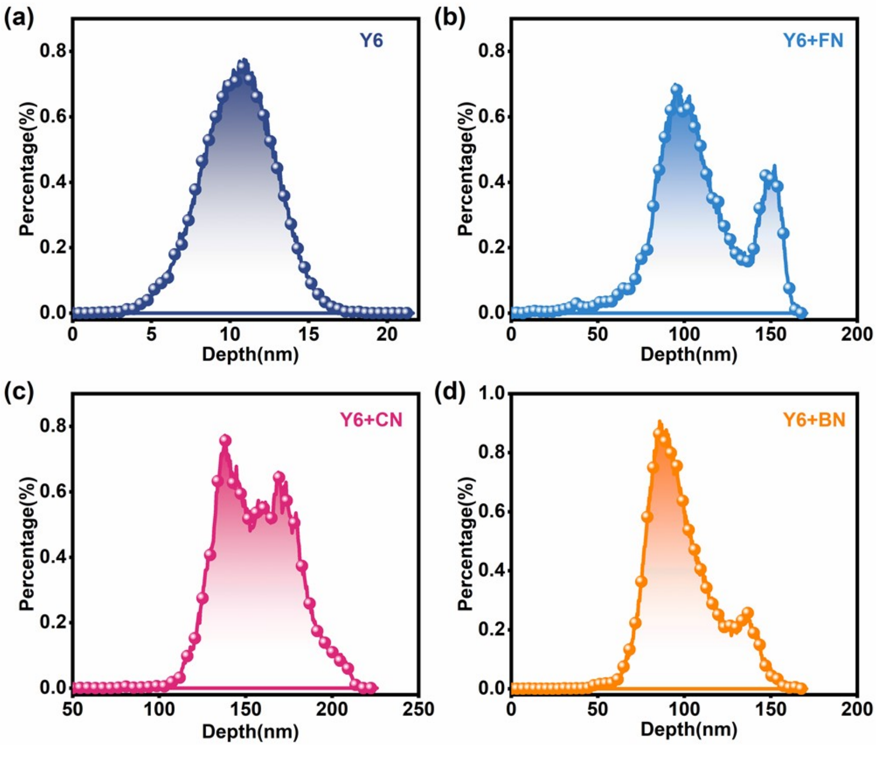

Figure S8. Depth of Y6 films changed with additives.

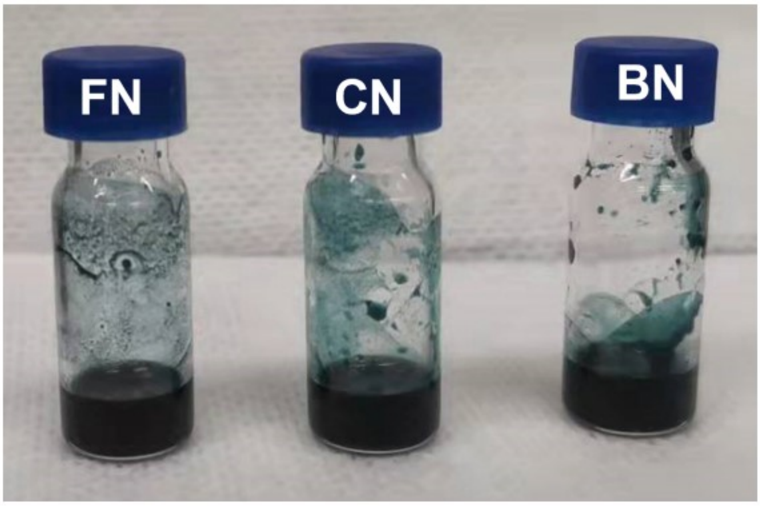

Figure S9. Saturated solutions of Y6 in 1-fluoronaphthalene (FN), 1-chloronaphthalene (CN), and 1-bromonaphthalene (BN) solvents.

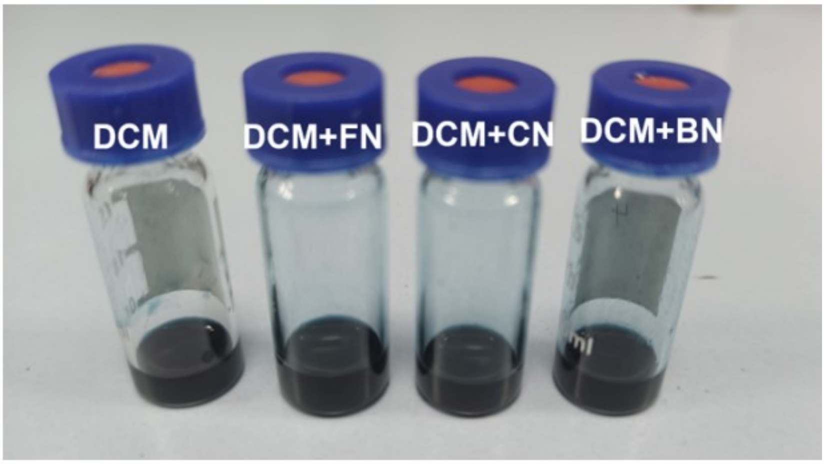

Figure S10. Saturated solutions of Y6 in DCM+FN, DCM+CN, and DCM+BN solvents.

Table S2. Solubility of Y6 in different solvents.

Solvents	Solubility (mg/ml)
FN	33.0
CN	70.0
BN	50.3
DCM	6.4
DCM+FN	6.9
DCM+CN	9.0
DCM+BN	7.5

6. AFM measurement of Y6 films with and w/o solid additives

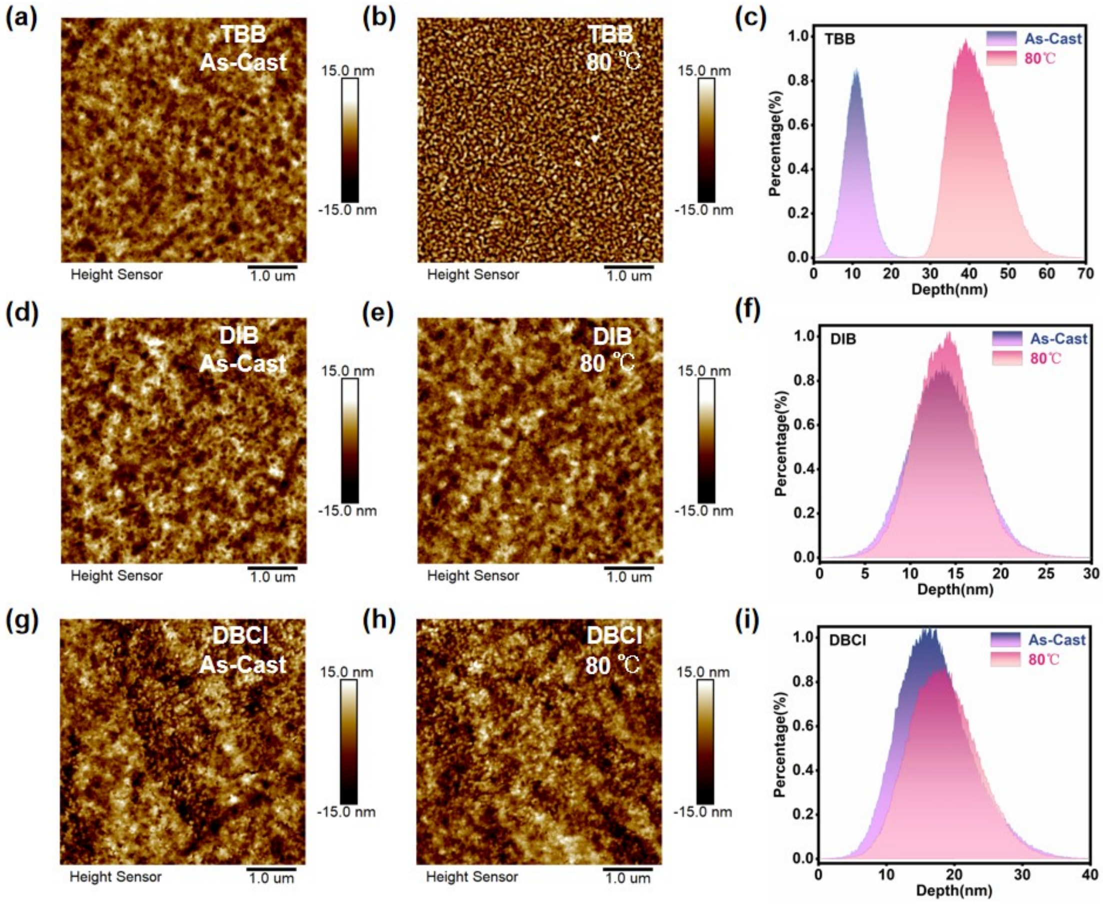

Figure S11. AFM topography of Y6 with and w/o solid additives.

7. J-V measurements of PM6/Y6 bilayer devices with and w/o solid additives

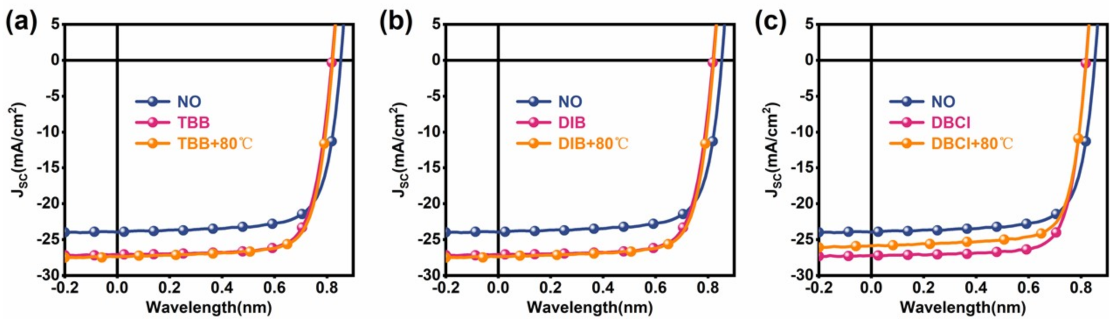

Figure S12. J-V curves of PM6/Y6 bilayer devices with and w/o additives.

Table S3. Photovoltaic parameters of PM6/Y6 bilayer OSCs with and w/o solid additives. The average values were obtained from 10 devices.

Post	Condition	J_{SC}(mA/cm^2)	V_{OC}(meV)	FF(%)	PCE(%)
As-Cast	None	25.15 (23.96±0.60)	856 (854±3)	75.02 (73.86±0.89)	16.15 (15.13±0.51)
	TBB	26.24 (25.44±1.34)	795 (793±18)	73.57 (73.39±1.00)	15.35 (14.78±0.55)
	DIB	27.08 (27.10±1.00)	819 (806±10)	75.43 (73.67±1.45)	16.73 (16.08±0.44)
	DBCl	27.61 (26.87±0.66)	793 (793±11)	73.76 (74.26±1.16)	16.16 (15.81±0.22)
Annealed by 90 °C	TBB	27.17 (25.41±1.46)	801 (808+20)	75.36 (75.57±1.18)	16.41 (15.50±0.58)
	DIB	27.38 (27.08±0.32)	822 (812±9)	75.56 (74.59±0.86)	17.00 (16.41±0.43)
	DBCl	25.85 (24.63±0.99)	820 (822±10)	75.40 (75.03±0.80)	15.98 (15.19±0.46)

8. AFM measurement of Y6 films in CF

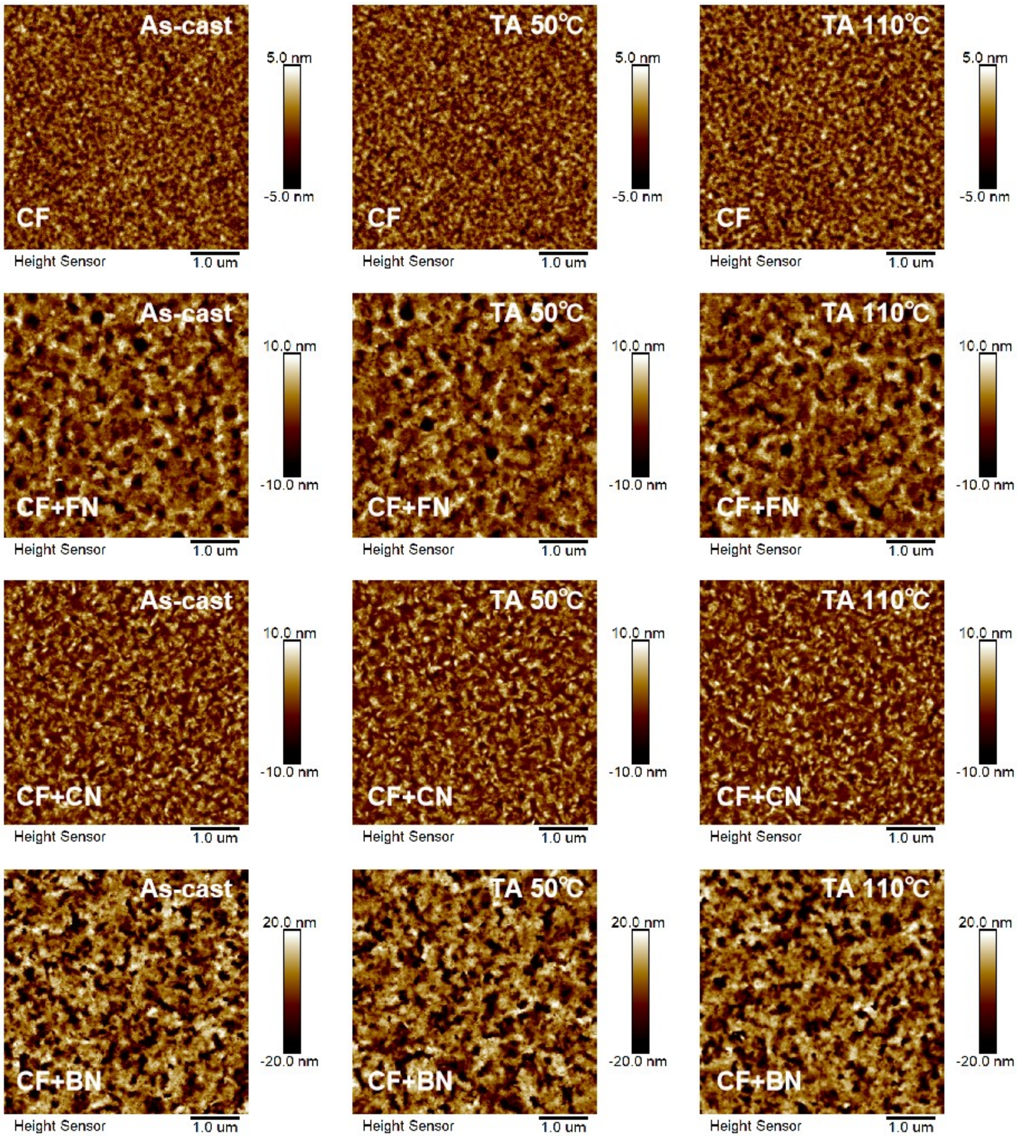

Figure S13. AFM topography of Y6 under different conditions with CF as the solvent.

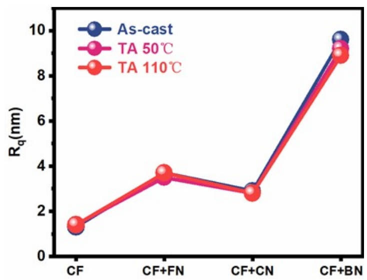

Figure S14. R_q of Y6 with CF as the solvent changed with additives and temperature.

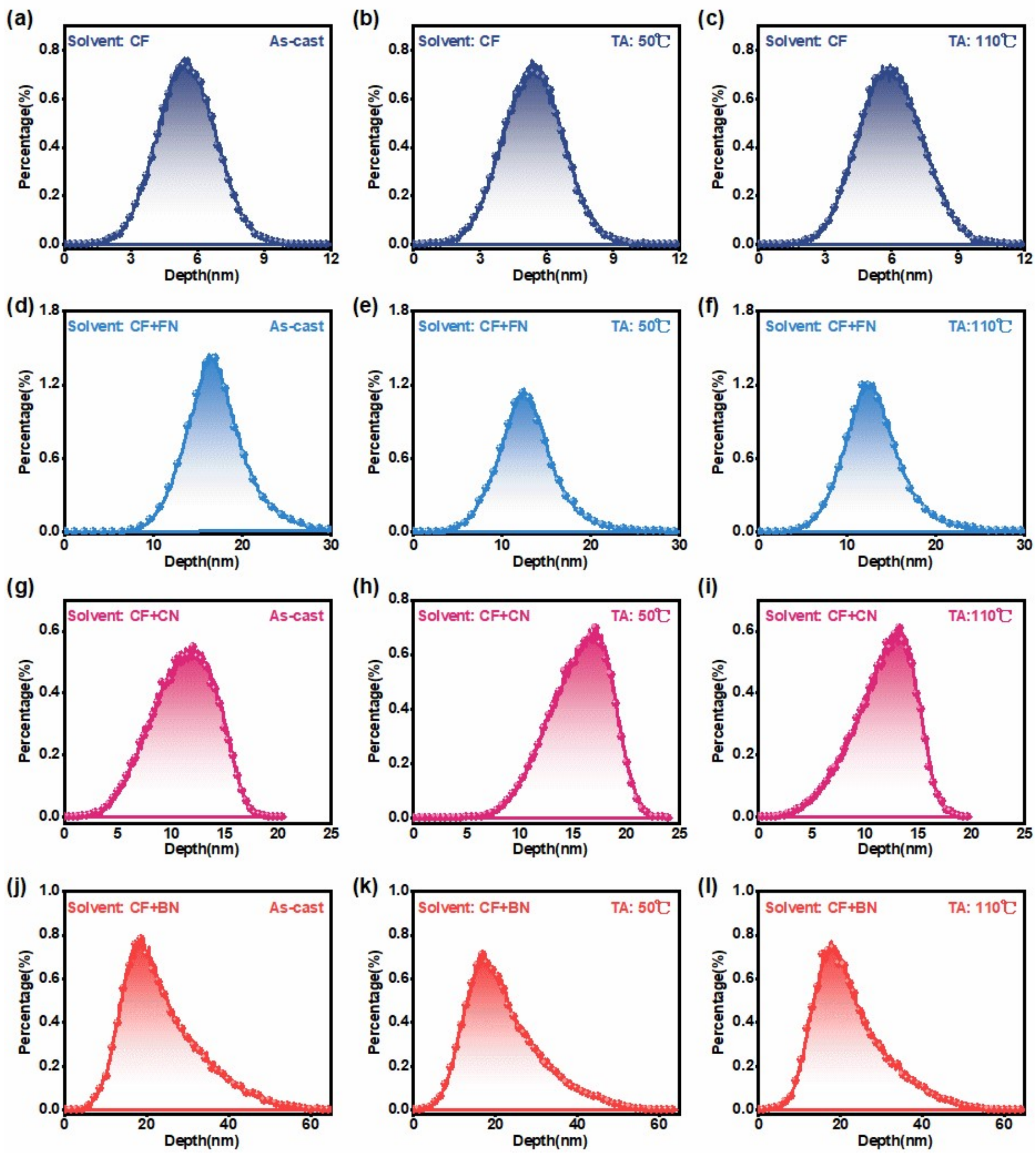

Figure S15. Depth of Y6 with CF as the solvent changed with additives and temperature.

9. J-V measurements of PM6:Y6 BHJ devices

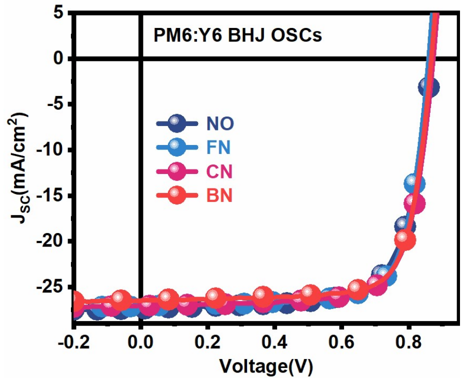

Figure S16. J-V spectra of PM6:Y6 BHJ devices with and w/o additives.

Table S4. Photovoltaic parameters of the optimized devices based on PM6:Y6 BHJ devices with and w/o additives under simulated AM1.5G illumination (100 mW cm-2). The average values were obtained from 10 devices.

Materials	Condition	V_{OC} (mV)	J_{SC} (mA/cm^2)	FF(%)	PCE (%)
PM6:Y6	None	862 (867±3)	27.79 (26.98±0.45)	72.05 (71.34±0.46)	17.25 (16.68±0.32)
	FN	859 (861±3)	27.05 (26.06±0.87)	75.50 (74.78±2.00)	17.54 (16.77±0.53)
	CN	873 (871±3)	27.03 (26.27±0.82)	74.76 (74.40±1.07)	17.65 (17.02±0.41)
	BN	868 (869±3)	26.50 (25.16±1.01)	76.11 (76.68±0.73)	17.50 (16.76±0.51)

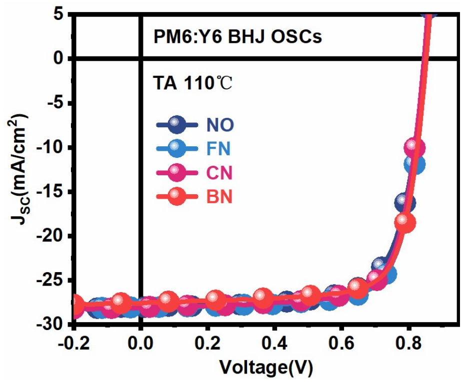

Figure S17. J-V spectra of PM6:Y6 BHJ devices with and w/o additives.

Table S5. Photovoltaic performance of the optimized devices based on PM6:Y6 BHJ devices with and w/o additives by annealing with 110°C under simulated AM1.5G illumination (100 mW cm^{-2}). The average values were obtained from 10 devices.

Materials	Condition	V_{OC} (mV)	J_{SC} (mA/cm^2)	FF(%)	PCE (%)
PM6:Y6 (TA 110°C)	As-cast	847 (867±6)	28.01 (27.46±0.53)	72.23 (71.80±1.39)	17.15 (16.62±0.34)
	FN	852 (843±7)	28.11 (27.51±0.70)	75.08 (74.67±1.16)	17.97 (17.32±0.45)
	CN	845 (843±2)	28.07 (27.28±0.61)	74.28 (74.08±0.86)	17.63 (17.03±0.30)
	BN	853 (845±4)	27.61 (26.39±0.66)	75.04 (75.30±0.90)	17.66 (16.79±0.43)

10. Absorbance spectra of Y6 films

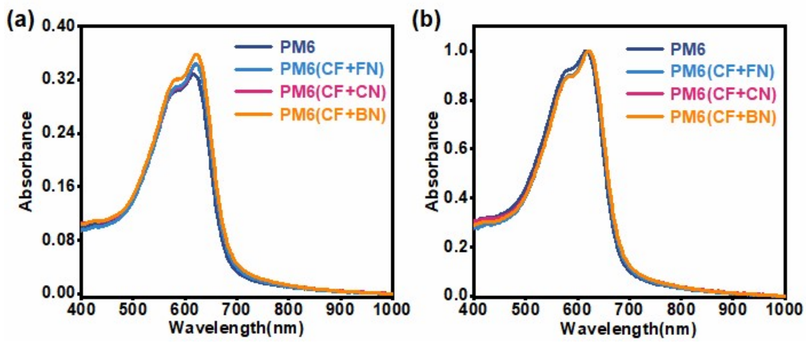

Figure S18. a) The absorbance spectra of PM6 with and w/o additives. **b)** The normalized absorbance spectra of PM6 with and w/o additives.

11. GIWAXS measurements of Y6

Grazing-incidence wide-angle X-ray scattering (GIWAXS) was carried out to investigate the molecular packing and molecular orientation in the thin films. The π–π stacking distance (d-spacing) and crystalline coherence length (CCL) were calculated quantitatively using the equations d-spacing = $2\pi/q$ and CCL = $2\pi K/\Delta q$, where q, Δq and the K constant represent the peak positions, full width at half maximum. [1,2]

Table S6 │ Peaks position of Y6 films in In-plane direction.

Peaks(Å^{-1})	None	FN	CN	BN
(100)	(0.35, 0)	(0.36, 0)	(0.33, 0)	(0.33, 0)
(001)	-	(0.28, 0)	(0.28, 0)	(0.28, 0)
(002)	-	(0.58, 0)	(0.58, 0)	(0.58, 0)
(003)	-	(0.90, 0)	(0.83, 0)	(0.82, 0)
(004)	-	(1.20, 0)	(1.23 0)	(1.20, 0)
(005)	-	(1.52, 0)	(1.44, 0)	(1.46, 0)

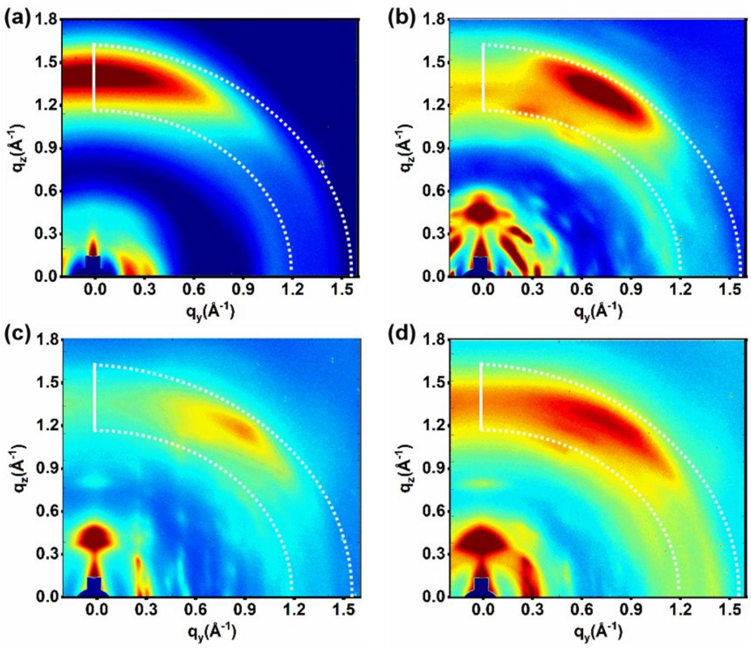

Figure S19. 2D-GIWAXS pattern of Y6 films cast from **a)** DCM, **b)** DCM with FN, **c)** DCM with CN, and **d)** DCM with BN.

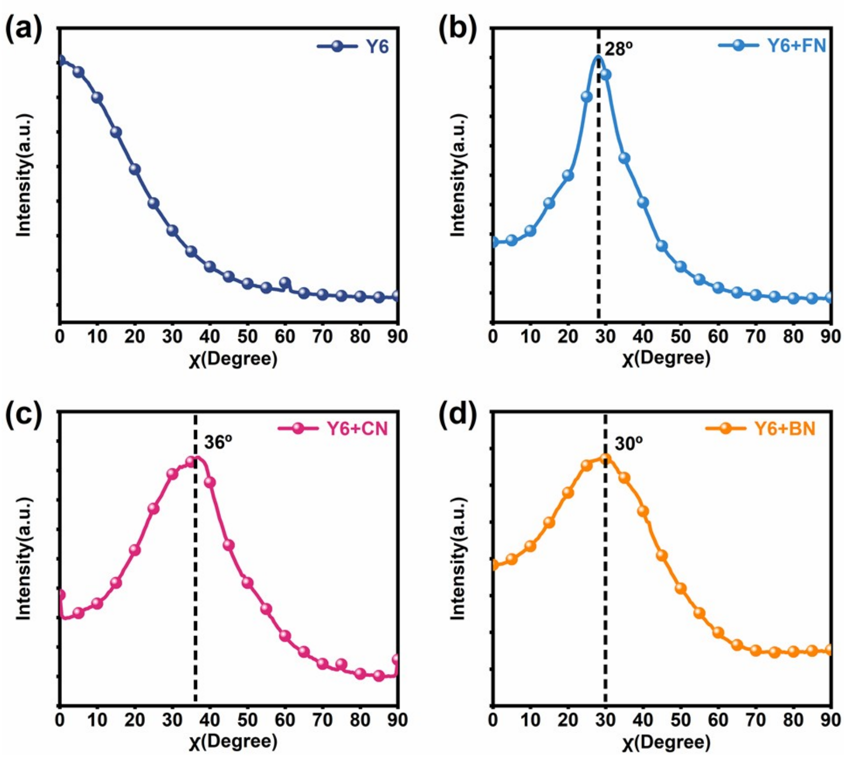

Figure S20. The corresponding polar intensity profiles extracted from the (010) diffraction of Y6 films.

12. GIWAXS measurements of PM6

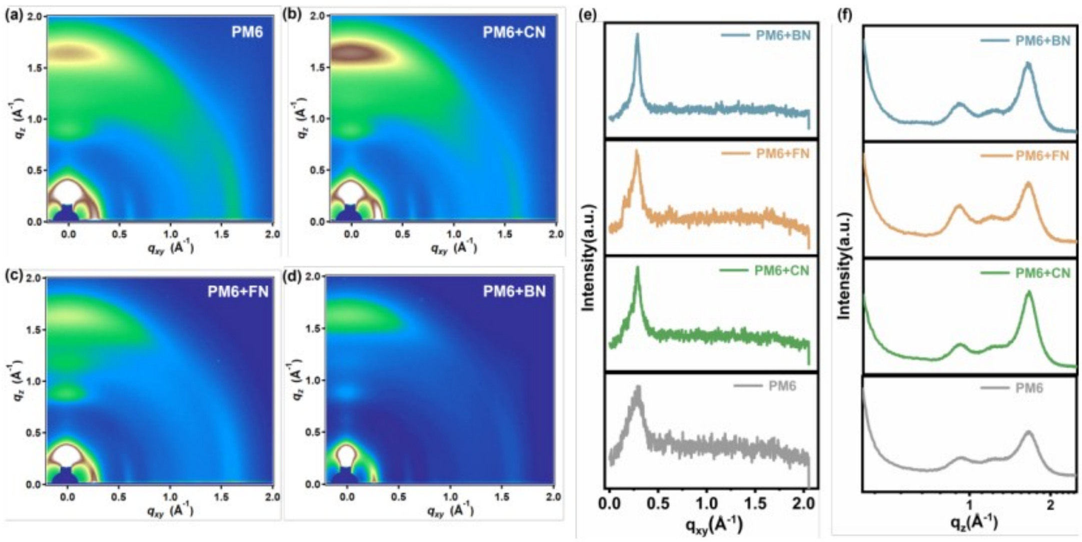

Figure S21. 2D-GIWAXS pattern of **a)** PM6, **b)** PM6+CN, **c)** PM6+FN and **d)** PM6+BN. **e)** In-plane and **f)** out-of-plane line cuts of the 2D-GIWAXS pattern.

Table S7 │ In-plane and out-of-plane parameters; peak location, d-spacing, FWHM, and crystal coherence length (CCL) extracted from the 2D GIWAXS of PM6 films.

Donor	**Peak**	**Peak location(Å^{-1})**	**d-space (Å)**	**FWHM(Å^{-1})**	**CCL(Å)**
PM6	IP(100)	0.28	22.35	0.10	58.27
	OOP(010)	1.66	3.79	0.23	24.36
PM6 (CN)	IP(100)	0.29	21.81	0.06	96.12
	OOP(010)	1.65	3.80	0.20	28.83
PM6 (FN)	IP(100)	0.28	22.43	0.08	74.46
	OOP(010)	1.64	3.83	0.24	24.05
PM6 (BN)	IP(100)	0.29	22.04	0.04	134.25
	OOP(010)	1.64	3.83	0.22	25.23

13. AFM measurements of PM6

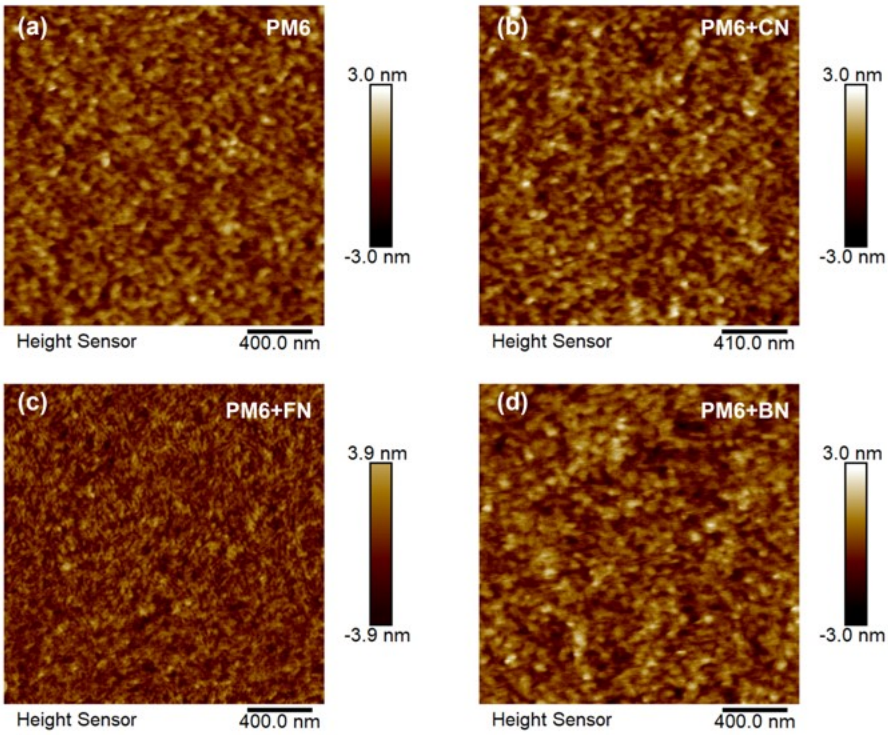

Figure S22. AFM topography of **a)** PM6, **b)** PM6+CN, **c)** PM6+FN and **d)** PM6+BN.

14. EQE Analyze

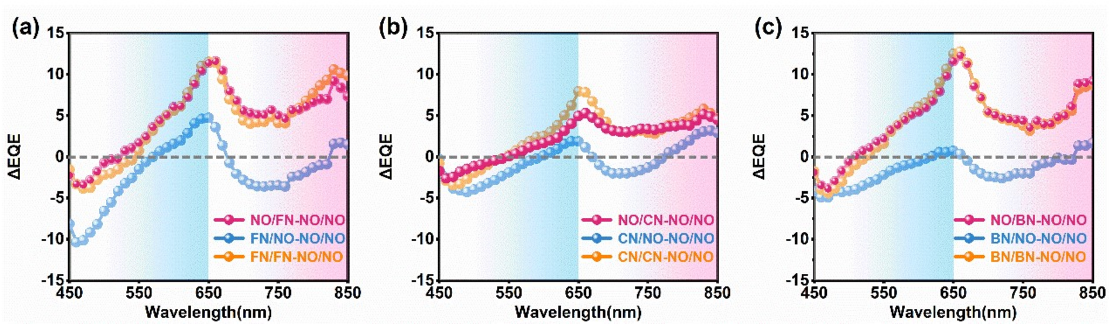

Figure S23. EQE spectra difference of devices with and w/o additives (ΔEQE).

15. Dark J-V measurements

The information on reverse saturated current ideality density, shunt resistance (R_{sh}), series resistance (R_s), and ideality factor (n) are derived from the dark J-V, the dark current density follows the following equation (the details are shown in Table S8) [3]:

$$J = J_0\left[exp(\frac{q(V-JR_s)}{nkT} - 1)\right] + \frac{V-JR_s}{R_{sh}}$$

Table S8 │Parameters of dark J-V measurements based on PM6/Y6 with and w/o additives.

Condition	n	R_s (Ohm cm^2)	R_{sh} (Ohm cm^2)
NO/NO	1.49±0.02	0.69±0.03	$7.97\times10^4\pm3.16\times10^3$
NO/CN	1.41±0.02	0.39±0.02	$6.77\times10^5\pm3.51\times10^4$
CN/NO	1.45±0.01	0.59±0.02	$7.86\times10^4\pm2.38\times10^3$
CN/CN	1.41±0.02	0.53±0.02	$9.97\times10^5\pm5.68\times10^4$
NO/FN	1.37±0.02	0.46±0.02	$6.49\times10^5\pm3.93\times10^4$
FN/NO	1.46±0.02	0.77±0.03	$1.24\times10^4\pm0.54\times10^3$
FN/FN	1.40±0.02	0.68±0.03	$4.93\times10^5\pm2.43\times10^4$
NO/BN	1.44±0.02	0.62±0.03	$5.16\times10^5\pm2.69\times10^4$
BN/NO	1.51±0.02	1.30±0.03	$5.18\times10^4\pm1.30\times10^3$
BN/BN	1.42±0.03	0.68±0.08	$2.69\times10^5\pm2.51\times10^4$

16. Photo-CLIEV measurements

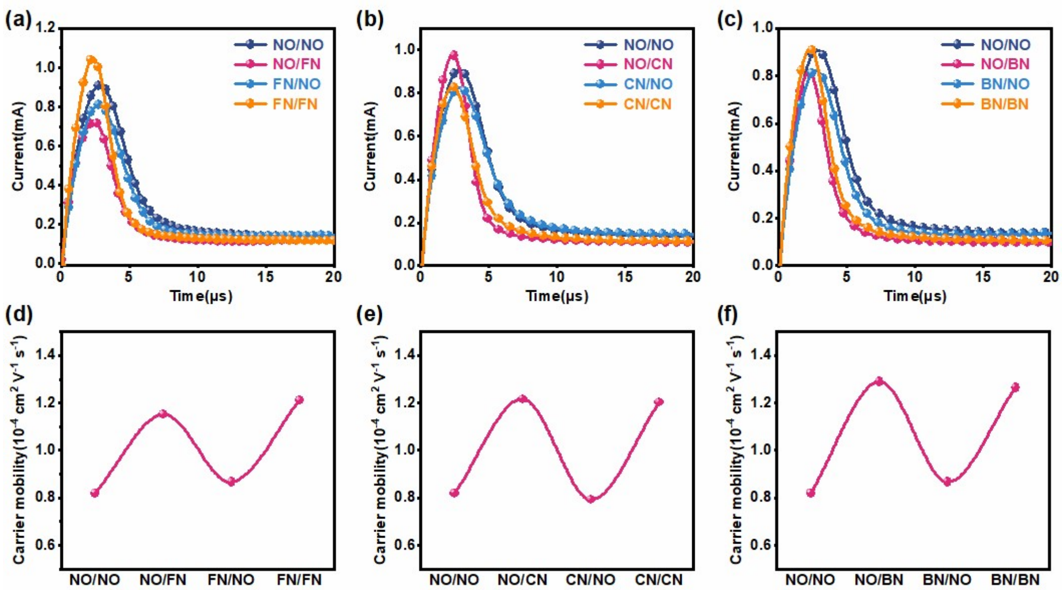

Figure S24. a-c) Photocurrent transient of PM6/Y6 bilayer devices with and w/o additives. **d-f)** Carrier mobility of PM6/Y6 bilayer devices change with additives.

17. DoS calculation

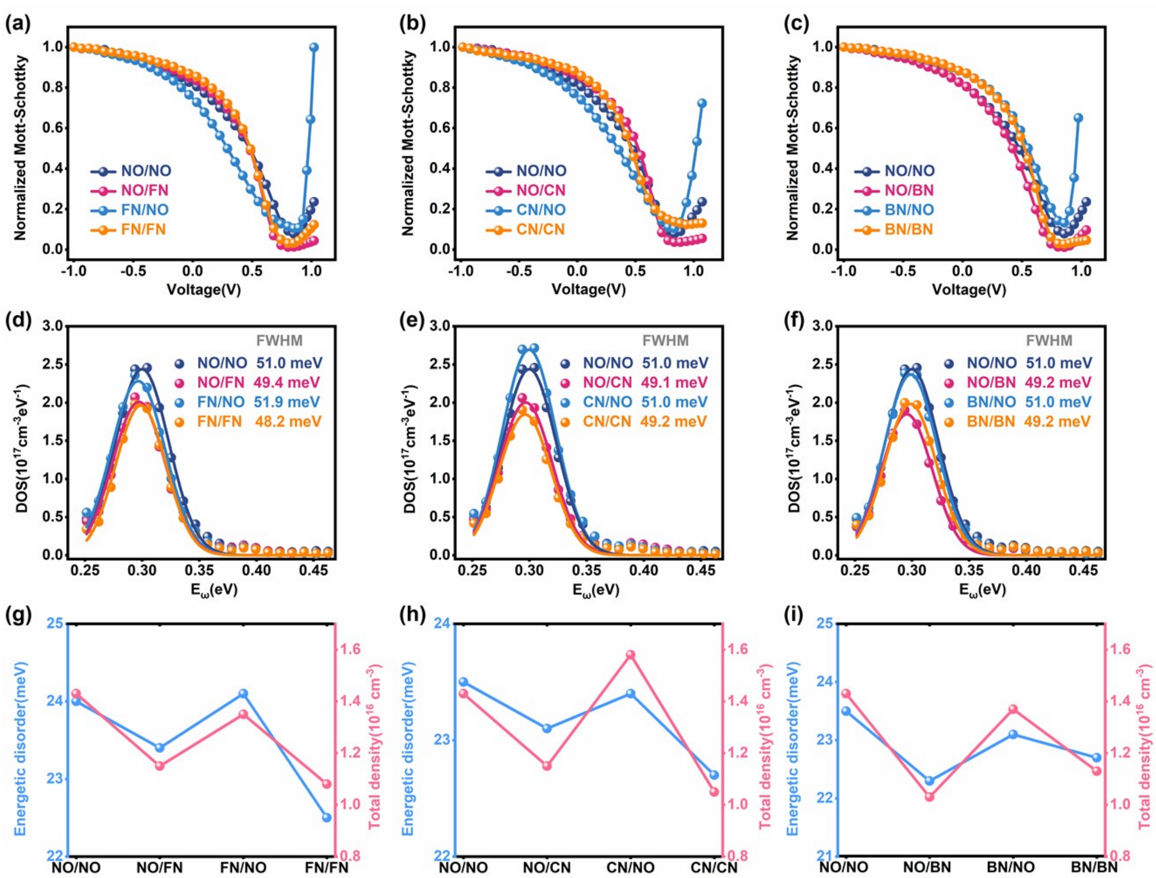

Figure S25. a-c) Mott-schottky spectra of devices based on PM6/Y6 with and w/o additives. **d-f)** DoS distribution of PM6/Y6 bilayer devices with and w/o additives. **g-i)** Energetic disorder (blue) and deep defect density (red) of PM6/Y6 bilayer devices change with additives.

The density of the state of trap distributions was performed through measurement of capacitance spectroscopy in a dark environment. In which, we applied capacitance-voltage (C-V) measurements under a frequency of 100 kHz at a different applied voltage from -1V to 1.2V (**Figure S25a**), and in the capacitance-frequency (C-f) measurement a varied frequency from 10 MHz to 10 Hz were used (**Figure S25b**).

The demarcation energy E_ω and modulation frequency ω are described as:

$$\omega = \omega_0 \exp\left(-\frac{\Delta E}{k_B T}\right) \tag{2}$$

with the solution of:

$$E_\omega = \mathrm{k_B T} ln(\frac{\omega_0}{\omega}) \tag{3}$$

The trap density at energy DoS (E_ω) can be acquired as:

$$\mathrm{DoS}(E_\omega) = -\frac{V_{bi}}{qW}\frac{dC}{d\omega}\frac{\omega}{\mathrm{k_B T}} \tag{4}$$

Where $\omega_0 = 2\pi\nu_0$ ($\nu_0 = 10^{12}$ s^{-1}) is called the attempt-to-escape frequency, W is the depletion width, $\frac{dC}{d\omega}$ is the derivative of each point in the capacitance with respect of AC frequency, n_t is the density of deep defect states, σ is the disorder parameter. [4,5]

18. Morphology of BTP-eC9

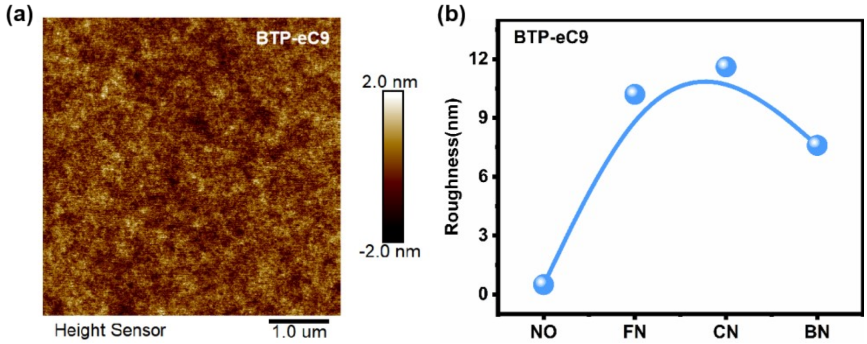

Figure S26. a) The AFM topography of the pristine BTP-eC9. **b)** R_q of BTP-eC9 changed with additives.

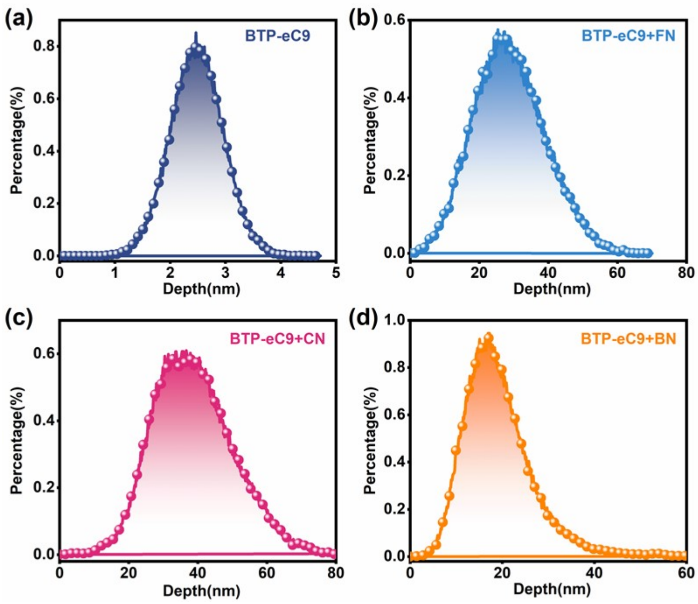

Figure S27. Depth of BTP-eC9 films changed with additives and temperature.

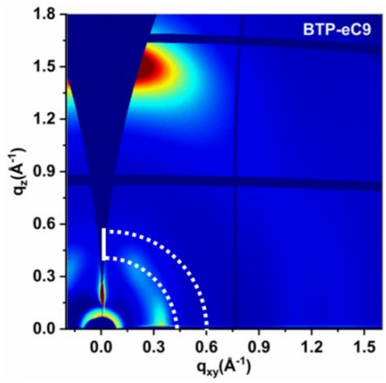

Figure S28. 2D GIWAXS pattern of the pristine BTP-eC9.

Table S9 │ Peaks position of BTP-eC9 films in In-plane direction.

Peaks($Å^{-1}$)	None	FN	CN	BN
(100)	(0.34, 0)	(0.31, 0)	(0.31, 0)	(0.35, 0)
(001)	-	(0.28, 0)	(0.28, 0)	(0.28, 0)
(002)	-	(0.55, 0)	(0.55, 0)	(0.49, 0)
(003)	-	(0.68, 0)	(0.68, 0)	(0.68, 0)
(004)	-	(0.93, 0)	(0.93, 0)	(0.93, 0)
(005)	-	(1.18, 0)	(1.18, 0)	(1.18, 0)
(006)	-	(1.55, 0)	(1.55, 0)	(1.55, 0)
(007)	-	(1.80, 0)	(1.80, 0)	(1.80, 0)

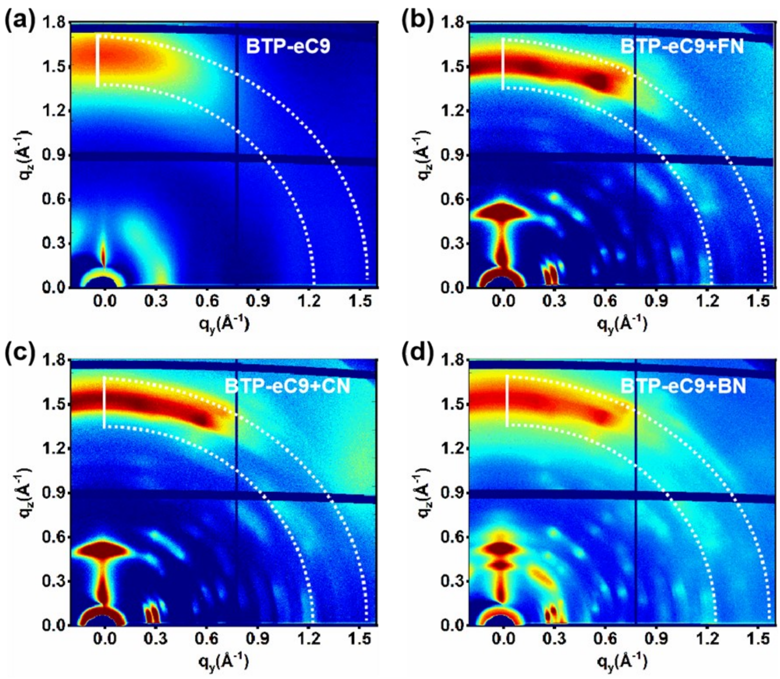

Figure S29. 2D-GIWAXS pattern of BTP-eC9 films cast from **a)** DCM, **b)** DCM with FN, **c)** DCM with CN, and **d)** DCM with BN.

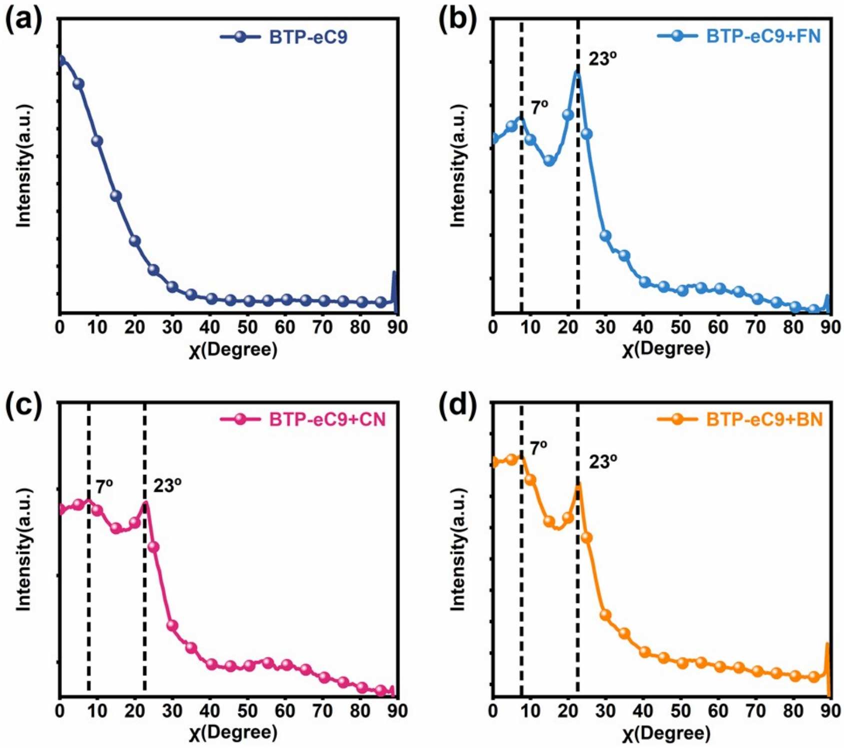

Figure S30. The corresponding polar intensity profiles extracted from the (010) diffraction of BTP-eC9 films.

19. Verification report of PM6/BTP-eC9(CN) bilayer devices

中国认可
国际互认
检测
TESTING
CNAS L8490

230017163974

Test and Calibration Center of New Energy Device and Module,
Shanghai Institute of Microsystem and Information Technology,
Chinese Academy of Sciences (SIMIT)

Measurement Report

Report No. 23TR101803

Client Name	Guangxi University, Zhipeng Kan's Group
Client Address	No.100, East Daxue Road, Nanning, Guangxi, China
Sample	Organic solar cell
Manufacturer	Guangxi University, Zhipeng Kan's Group
Measurement Date	18th October, 2023

Performed by:	Qiang Shi Qiang Shi	**Date:** 19/10/2023
Reviewed by:	Wenjie Zhao Wenjie Zhao	**Date:** 18/10/2023
Approved by:	Yucheng Liu Yucheng Liu	**Date:** 18/10/2023

Address: No.235 Chengbei Road, Jiading, Shanghai **Post Code:**201800
E-mail: solarcell@mail.sim.ac.cn **Tel:** +86-021-69976921

The measurement report without signature and seal are not valid.
This report shall not be reproduced, except in full, without the approval of SIMIT.

1 / 3

Sample Information

Sample Type	Organic solar cell
Serial No.	17-1-3#
Lab Internal No.	23101801-3#
Measurement Item	I-V characteristic
Measurement Environment	24.6±2.0°C,49.1±5.0%R.H

Measurement of I-V characteristic

Reference cell	PVM 1121
Reference cell Type	mono-Si, WPVS, calibrated by NREL (Certificate No. ISO 2075)
Calibration Value/Date of Calibration for Reference cell	144.53mA/ Feb. 2023
Measurement Conditions	Standard Test Condition (STC): Spectral Distribution: AM1.5 according to IEC 60904-3 Ed.3, Irradiance: 1000±50W/m^2, Temperature: 25±2°C
Measurement Equipment/ Date of Calibration	AAA Steady State Solar Simulator (YSS-T155-2M) / July.2023 IV test system (ADCMT 6246) / June. 2023 Measuring Microscope (MF-B2017C) / July.2023
Measurement Method	I-V Measurement: Dual-lamp solar simulator spectral distribution adjusted to mask the match factor within 1.00±0.01; Logarithmic sweep in both directions (Isc to Voc and Voc to Isc) during one flash based on IEC 60904-1:2020.
Measurement Uncertainty	Area: 1.0%(k=2); Isc: 1.9%(k=2); Voc: 1.0%(k=2); Pmax: 2.4%(k=2); Eff: 2.5%(k=2)

====Measurement Results ====

	Forward Scan (Isc to Voc)	Reverse Scan (Voc to Isc)
Area	3.64 mm²	
Isc	1.011 mA	1.011 mA
Voc	0.860 V	0.861 V
Pmax	0.661 mW	0.662 mW
Ipm	0.920 mA	0.922 mA
Vpm	0.718 V	0.718 V
FF	75.99 %	76.00 %
Eff	18.15 %	18.17 %

- Designated illumination area defined by a thin mask was measured by measuring microscope.
- Test results listed in this measurement report refer exclusively to the mentioned measured sample.
- The results apply only at the time of the test, and do not imply future performance.

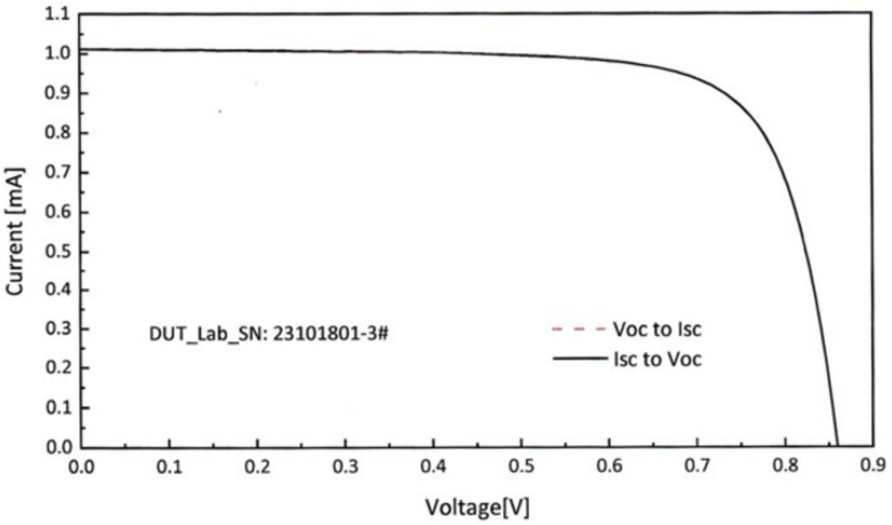

Fig.1 I-V curves of the measured sample

-------End of Report-------

20. Verification report of PM6/Y6(CN) bilayer devices

中国认可
国际互认
检测
TESTING
CNAS L8490

230017163974

Test and Calibration Center of New Energy Device and Module,
Shanghai Institute of Microsystem and Information Technology,
Chinese Academy of Sciences (SIMIT)

Measurement Report

Report No. 23TR101802

Client Name	Guangxi University, Zhipeng Kan's Group
Client Address	No.100, East Daxue Road, Nanning, Guangxi, China
Sample	Organic solar cell
Manufacturer	Guangxi University, Zhipeng Kan's Group
Measurement Date	18th October, 2023

Performed by:	Qiang Shi *Qiang Shi*	**Date:** 18/10/2023
Reviewed by:	Wenjie Zhao *Wenjie Zhao*	**Date:** 18/10/2023
Approved by:	Yucheng Liu *Yucheng Liu*	**Date:** 18/10/2023

Address: No.235 Chengbei Road, Jiading, Shanghai **Post Code:**201800

E-mail: solarcell@mail.sim.ac.cn **Tel:** +86-021-69976921

The measurement report without signature and seal are not valid.
This report shall not be reproduced, except in full, without the approval of SIMIT.

1 / 3

SiMIT

Report No. 23TR101802

Sample Information

Sample Type	Organic solar cell
Serial No.	10-1-5#
Lab Internal No.	23101801-2#
Measurement Item	I-V characteristic
Measurement Environment	24.6±2.0°C,49.1±5.0%R.H

Measurement of I-V characteristic

Reference cell	PVM 1121
Reference cell Type	mono-Si, WPVS, calibrated by NREL (Certificate No. ISO 2075)
Calibration Value/Date of Calibration for Reference cell	144.53mA/ Feb. 2023
Measurement Conditions	Standard Test Condition (STC): Spectral Distribution: AM1.5 according to IEC 60904-3 Ed.3, Irradiance: 1000±50W/m², Temperature: 25±2°C
Measurement Equipment/ Date of Calibration	AAA Steady State Solar Simulator (YSS-T155-2M) / July.2023 IV test system (ADCMT 6246) / June. 2023 Measuring Microscope (MF-B2017C) / July.2023
Measurement Method	I-V Measurement: Dual-lamp solar simulator spectral distribution adjusted to mask the match factor within 1.00±0.01; Logarithmic sweep in both directions (Isc to Voc and Voc to Isc) during one flash based on IEC 60904-1:2020.
Measurement Uncertainty	Area: 1.0%(k=2); Isc: 1.9%(k=2); Voc: 1.0%(k=2); Pmax: 2.4%(k=2); Eff: 2.5%(k=2)

====**Measurement Results** ====

	Forward Scan (Isc to Voc)	Reverse Scan (Voc to Isc)
Area	3.64 mm^2	
Isc	0.961 mA	0.960 mA
Voc	0.861 V	0.861 V
Pmax	0.637 mW	0.637 mW
Ipm	0.882 mA	0.883 mA
Vpm	0.722 V	0.721 V
FF	76.94 %	77.02 %
Eff	17.50 %	17.50 %

- Designated illumination area defined by a thin mask was measured by measuring microscope.
- Test results listed in this measurement report refer exclusively to the mentioned measured sample.
- The results apply only at the time of the test, and do not imply future performance.

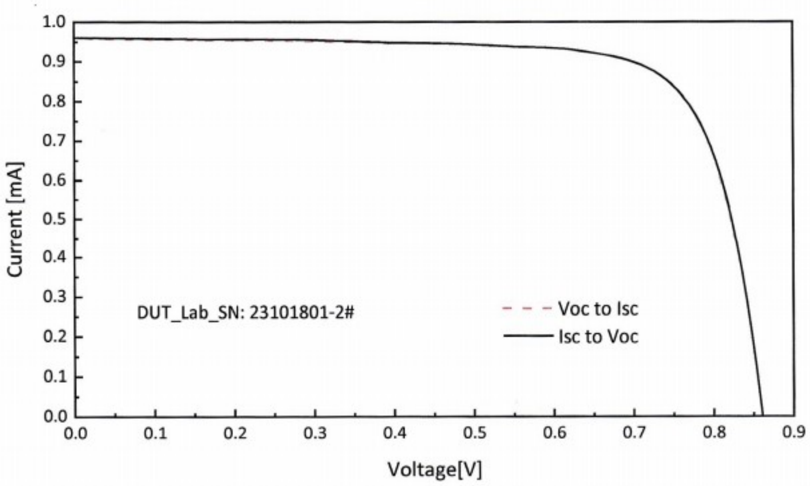

Fig.1 I-V curves of the measured sample

-------**End of Report**-------

21. References

(1) Qin, Y. et al. Low Temperature Aggregation Transitions in N3 and Y6 Acceptors Enable Double-Annealing Method That Yields Hierarchical Morphology and Superior Efficiency in Nonfullerene Organic Solar Cells. *Adv. Funct. Mater. 30,* 2005011 (2020).

(2) Sun, R. et al. A Layer-by-Layer Architecture for Printable Organic Solar Cells Overcoming the Scaling Lag of Module Efficiency. *Joule.* **4,** 407-419 (2020).

(3)Ortiz-Conde, A. et al. Exact analytical solutions of the forward non-ideal diode equation with series and shunt parasitic resistances. *Solid-State Electronics.* **44,** 1861-1864 (2000).

(4) Ni, Z. et al. Resolving spatial and energetic distributions of trap states in metal halide perovskite solar cells. *Science.* **367,** 1352–1358 (2020).

(5) Jiang, K. et al. Alkyl chain tuning of small molecule acceptors for efficient organic solar cells. *Joule.* **3,** 3020-3033 (2019).